

A three-phase state estimation in active distribution networks



Aleksandar Ranković^{a,*}, Branko M. Maksimović^b, Andrija T. Sarić^{a,c}

^a Faculty of Technical Sciences, University of Kragujevac, Čačak, Serbia

^b Technical High School, Čačak, Serbia

^c Faculty of Technical Sciences, University of Novi Sad, Novi Sad, Serbia

ARTICLE INFO

Article history:

Received 28 May 2012

Received in revised form 4 July 2013

Accepted 5 July 2013

Keywords:

Distribution network

State estimation

Three-phase algorithm

Weighted Least Square (WLS) algorithm

Distributed generation

ABSTRACT

This paper presents the improved Weighted Least Square (WLS) based three-phase state estimation algorithm for active distribution networks. The three-phase component models are developed for characteristic types of transformers (respecting their winding connections), lines (three and four wires), loads (voltage dependent grounded-Y, ungrounded-Y and ungrounded- Δ) and distributed generation (DG) units (synchronous generator, induction generator and three-phase (three- and four-wire) electronically-coupled based DG units). The unmonitored (or partially monitored) powers of loads and DG units are initially estimated from normalized daily load profiles, or from external inputs (historical database/weather forecast), such as wind, sun and water inflow forecasts, respectively. These measurements are introduced with lower weights (treated as the pseudo-measurements in the proposed state estimation algorithm). The results and practical aspects of the proposed methodology are demonstrated on two characteristic examples: modified IEEE 13-bus test system and 322-bus real-world distribution network.

© 2013 Elsevier Ltd. All rights reserved.

1. Introduction

State estimation (SE) is mainly used to filter the noise (random error) of redundant measurements and other data and provide a reliable SE of the transmission or distribution network [1]. The SE in distribution networks is usually based on a limited number of real-time measurements. The distribution networks consist mainly of radial, short and un-transposed feeders with high R/X ratios and with single-, two- or three-phase laterals, and loads along the feeders that usually can be single- and two-phase for residential customers, or three-phase for both commercial and industrial customers. Therefore, the distribution networks are unbalanced in general. Furthermore, even if the distribution network is balanced, the asymmetrical faults additionally introduce an imbalance. This means that the proposed three-phase SE model is interesting for both normal and emergency conditions. To avoid the significant error arising from the inherent network imbalance, the detailed component models are required for SE in distribution networks in both normal and contingency operation conditions. Note that by respecting the above mentioned characteristics of the distribution networks, the decoupled Weighted Least Square (WLS) based algorithms are not suitable for their SE [2–5].

Since the number of consumers and distributed generators (DGs) connected to a distribution network may be large, it is

impractical to telemeter all points of the network. However, a practical distribution networks should have the following features and types of measurements that are available [6–10]:

- *Substation measurements*: Several types of real-time measurements are available at the source or distribution substations (bus real/reactive power injections/feeder flows, bus voltage magnitudes, bus current injection/feeder flow magnitudes, and circuit breaker statuses).
- *Few measurements on critical points of the network*: Any affordable measurements need to be placed on the critical points in the network to reduce the standard deviation of the computed state variables or provide the network observability.
- *Customer load estimates*: They are usually available for large number of unmeasured buses remote from the source substation. In general, the observability of the distribution network is achieved using these pseudo-measurements.
- *DG unit measurements/estimates*: They are usually provided with bus voltage and real power injection real-time measurements. The unavailable real-time measurements at unmonitored DG units can be replaced with pseudo-measurements obtained from the external inputs (historical database and/or weather forecast).

Based on previously published references we can draw a conclusion that for unbalanced transmission and distribution power networks the three-phase power flow [11–16] is more frequently explored problem than the three-phase SE [17–19].

* Corresponding author. Tel.: +381 32 302 761; fax: +381 32 342 101.

E-mail address: aleksandar.rankovic@ftn.kg.ac.rs (A. Ranković).

Only few previously proposed three-phase SE algorithms can be adopted for unbalanced distribution networks [2–5,15]. A common feature of the previously proposed distribution SE algorithms is that they are based on the modification of the WLS-based single-phase SE algorithms originally developed for transmission networks, or minimally adopted for radial (meshed) distribution networks. However, in previously proposed algorithms all the problems which pertain to the SE in modern distribution networks are not resolved in general, respecting the following shortcomings:

- Due to an imbalance of the distribution system operating conditions, the complete and accurate three-phase models are desirable for distribution and inline transformers of various core and winding configurations.
- Detailed models of (un-)grounded Y- and Δ -connected nonlinear loads are usually replaced with the simple constant phase PQ injection bus model.
- The DG units are usually modeled by PQ (PV) bus injection model, without detailed modeling of the DG units. It is important to note that determining a suitable model for each DG unit in SE of the distribution networks requires the knowledge of the DG operation and the type of its connection to the grid (direct or indirect connection).

Based on the previous considerations, the improved three-phase SE algorithm is proposed in this paper with the following features included:

- Detailed transformer models including copper and core losses, winding connection and phase-shifting between primary and secondary windings. An individual phase representation is used, as opposed to a balanced three-phase model.
- Line models for both coupled and uncoupled feeders.
- Loads can be a combination of constant current, constant power, and constant admittance models. They may be either (un-)grounded Y- or Δ -connected.
- The significance of the DG model presented here stems from the inclusion of the inherent phase imbalance caused by the distribution network operating imbalances. The DGs can be either directly connected synchronous or induction generator, as well as three-phase electronically-coupled DG units, and can be on either primary or secondary systems.
- Different types of monitored, partially monitored or unmonitored DG units and loads are included in the SE algorithm. The initial internal powers for unmonitored (partially monitored) DG units are calculated on the basis of external inputs, such as wind, sun and water inflow forecasts (depending on the type of DG unit), or from the historical database and from the normalized daily load profiles for loads.

The proposed methodology was verified on two characteristic test power examples: (1) modified IEEE 13-bus test system and (2) 322-bus real-world distribution network.

This paper is organized as follows. Section 2 presents the three-phase models of transformers, lines, loads and DG units. Section 3 explains the interaction among state variables, bus (or full network) observability and adopted pseudo-measurements in order to provide the full network observability. Section 4 describes in more details the WLS-based three-phase SE algorithm in active distribution networks. The final part of the paper presents simulation results (in Section 5) and main derived conclusions (in Section 6). The details about used three-phase transformer models are provided Appendix A.

2. Component three-phase models

The matrix equation that is used to describe the three-phase distribution network in admittance form is

$$\underline{I} = \underline{Y}_{BUS}\underline{V}, \quad (1)$$

where \underline{I} , \underline{V} is the $(3N)$ -dimensional vectors of bus phase currents and voltages, respectively (N is total number of buses in distribution network) and \underline{Y}_{BUS} is the $(3N) \times (3N)$ -dimensional bus admittance matrix.

Characteristic types of the distribution network elements in the current–voltage model (1), such as transformers, lines, loads and DG units, are derived in the following subsections.

2.1. Transformers

By eliminating the neutral point with Kron reduction, the resulting transformer bus admittance matrix (\underline{Y}_T) can be reduced to (6×6) -dimensional [11,12,19]. The general three-phase transformer model is shown on Fig. 1.

By using the transformer bus admittance matrix \underline{Y}_T in Fig. 1, the three-phase transformer current–voltage relationship between transformer primary (p) and secondary (s) sides can be expressed as

$$\begin{bmatrix} \underline{I}_p \\ \underline{I}_s \end{bmatrix} = \begin{bmatrix} \underline{Y}_{pp} & \underline{Y}_{ps} + \underline{Y}_m \\ \underline{Y}_{sp} & \underline{Y}_{ss} + \underline{Y}_m \end{bmatrix} \begin{bmatrix} \underline{V}_p \\ \underline{V}_s \end{bmatrix}, \quad (2)$$

where \underline{Y}_{pp} , \underline{Y}_{ps} , \underline{Y}_{sp} , \underline{Y}_{ss} is the (3×3) -dimensional submatrices defined in Appendix A and \underline{Y}_m is the (3×3) -dimensional magnetizing admittance matrix, calculated as [19]

$$\underline{Y}_m = \underline{A}\underline{Y}_m^{012}\underline{A}^{-1} = \frac{1}{3} \begin{bmatrix} 2\underline{Y}_m^1 + \underline{Y}_m^0 & -\underline{Y}_m^1 + \underline{Y}_m^0 & -\underline{Y}_m^1 + \underline{Y}_m^0 \\ -\underline{Y}_m^1 + \underline{Y}_m^0 & 2\underline{Y}_m^1 + \underline{Y}_m^0 & -\underline{Y}_m^1 + \underline{Y}_m^0 \\ -\underline{Y}_m^1 + \underline{Y}_m^0 & -\underline{Y}_m^1 + \underline{Y}_m^0 & 2\underline{Y}_m^1 + \underline{Y}_m^0 \end{bmatrix}, \quad (3)$$

where \underline{A} is the Fortescue transformation matrix; $\underline{Y}_m^{012} = \text{diag}\{\underline{Y}_m^0, \underline{Y}_m^1, \underline{Y}_m^2\}$; $\underline{Y}_m^1 = \underline{Y}_m^2$ the positive (equal with negative) sequence transformer magnetizing admittance; and \underline{Y}_m^0 is the zero sequence transformer magnetizing admittance (different from zero only for grounded-Y on secondary transformer side, where this admittance formally is assigned - see Fig. 1).

2.2. Lines

In this paper, the lines are modeled as the multi-grounded three-phase four-wire line sections. After applying Kron reduction technique [19], the general three-phase line model is shown in Fig. 2. From this figure, the line three-phase current–voltage relationship can be expressed as

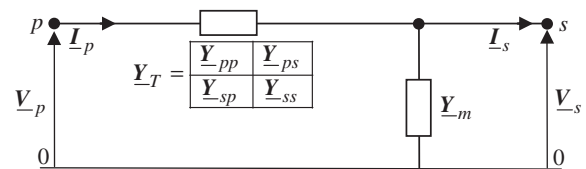


Fig. 1. General three-phase transformer model.

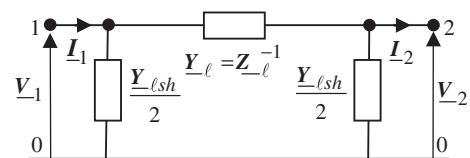


Fig. 2. General three-phase line model.

$$\begin{bmatrix} \mathbf{I}_1 \\ \mathbf{I}_2 \end{bmatrix} = \begin{bmatrix} \mathbf{Y}_\ell + \mathbf{Y}_{sh}/2 & -\mathbf{Y}_\ell \\ -\mathbf{Y}_\ell & \mathbf{Y}_\ell + \mathbf{Y}_{sh}/2 \end{bmatrix} \begin{bmatrix} \mathbf{V}_1 \\ \mathbf{V}_2 \end{bmatrix}, \quad (4)$$

where

$$\mathbf{Y}_\ell = \begin{bmatrix} Y_{aa} & Y_{ab} & Y_{ac} \\ Y_{ab} & Y_{bb} & Y_{bc} \\ Y_{ac} & Y_{bc} & Y_{cc} \end{bmatrix} = \mathbf{Z}_\ell^{-1} = \begin{bmatrix} Z_{aa} & Z_{ab} & Z_{ac} \\ Z_{ab} & Z_{bb} & Z_{bc} \\ Z_{ac} & Z_{bc} & Z_{cc} \end{bmatrix}^{-1}, \quad (5)$$

\mathbf{Y}_ℓ (\mathbf{Z}_ℓ), \mathbf{Y}_{sh} is the (3×3) -dimensional three-phase series admittance (impedance) and shunt admittance matrices, respectively; for the calculation of particular elements, see [19-Sections 4, 5].

2.3. Loads

Loads can be represented as a combination of constant power, constant current, and constant admittance models. Those same loads may be either Y- or Δ -connected. It is assumed that for load (L) \mathbf{V}_L is the three-phase voltage ($\mathbf{V}_L = [V_{La} \ V_{Lb} \ V_{Lc}]^T$), \mathbf{I}_L is the three-phase load current ($\mathbf{I}_L = [I_{La} \ I_{Lb} \ I_{Lc}]^T$) and \mathbf{Y}_L is (3×3) -dimensional admittance matrix. Therefore, there are the following specific load models [20]:

- **Grounded-Y:** All grounded-Y connected loads can be modeled as a combination of the following models:

$$(1) \text{ Constant power : } \mathbf{S}_L = [\underline{S}_{La} \ \underline{S}_{Lb} \ \underline{S}_{Lc}]^T = \mathbf{I}_L^* \times \mathbf{V}_L; \quad (6)$$

$$(2) \text{ Constant current : } \mathbf{I}_L = [I_{La} \ I_{Lb} \ I_{Lc}]^T; \quad (7)$$

$$(3) \text{ Constant admittance : } \mathbf{I}_L = \mathbf{Y}_L \mathbf{V}_L, \quad (8)$$

where \times in (6) denotes element-wise operation.

The model of real/reactive loads for phases a , b and c is a combination of constant power (S), constant current (I) and constant admittance (Y) models, respectively:

$$\underline{S}_{Lx} = k_{PSx} P_{Lxn} + k_{PIx} \frac{V_{Lx}}{V_{Ln}} P_{Lxn} + k_{PYx} \left(\frac{V_{Lx}}{V_{Ln}} \right)^2 P_{Lxn} + j \left[k_{QSx} Q_{Lxn} + k_{QIx} \frac{V_{Lx}}{V_{Ln}} Q_{Lxn} + k_{QYx} \left(\frac{V_{Lx}}{V_{Ln}} \right)^2 Q_{Lxn} \right]; \quad x = a, b, c, \quad (9)$$

where P_{Lxn} (Q_{Lxn}) denote the real (reactive) load on the rated voltage, while the participation factors for real and reactive powers respectively satisfy the following conditions:

$$k_{PSx} + k_{PIx} + k_{PYx} = 1.0; \quad k_{QSx} + k_{QIx} + k_{QYx} = 1.0. \quad (10)$$

Both **ungrounded-Y** and **ungrounded- Δ** connected loads can be modeled in a similar fashion as above described **grounded-Y** configuration [20].

2.4. Distributed generation (DG) units

Different types of the DG units and a way for their connection to the grid are summarized in Table 1 (including sections in which the models are described in more details) [21,22].

Based on the presented overview of the DG unit types (Table 1), the following models are adopted.

2.4.1. Synchronous generator (SG) with round-rotor [11,23]

The SGs that are driven by steam turbines (turbo-generators) have cylindrical (round) rotors with slots in which distributed field windings are placed. The SGs can be modeled by Thevenin equivalent circuit with an internal source voltage (E_i) behind the generator's impedance in d -axis only in a positive sequence circuit ($\underline{Z}_g^1 = \underline{Z}_d$). This model is different from the traditional power flow

Table 1
Types of the DG units and a way for their connection to the grid.

DG unit	Way of connection	Section
Small- and medium-scale hydro turbines	Synchronous generator (SG) with salient-poles (directly connected to the grid)	2.4.2
Micro-scale hydro turbines	Induction generator (IG) (directly connected to the grid)	2.4.3
Wind turbines with variable speed	Doubly fed IG (SG) (connected to the grid by voltage-sourced converter (VSC))	2.4.4
Wind turbines with fixed speed	Squirrel cage IG (directly connected to the grid)	2.4.3
Photovoltaic systems	VSC	2.4.4
Internal combustion engines	SG with round-rotor, or IG (directly connected to the grid)	2.4.1, or 2.4.3
Fuel cells	VSC	2.4.4
Gas turbines	SG with round-rotor (directly connected to the grid)	2.4.1
Micro-turbines	High-speed permanent magnet SG (connected to the grid by VSC)	2.4.4

based PV bus model, which is represented by the specified injected real power and bus voltage where the DG is connected to the grid.

The Thevenin equivalent sequence circuits can be converted to Norton equivalent sequence circuits, as shown in Fig. 3, where the current source is used only in positive sequence circuit ($I_g^1 = I_L$) instead of the internal source voltage (E_i), while zero, positive and negative sequence admittances are respectively:

$$\underline{Y}_g^0 = 1/(\underline{Z}_g^0 + 3\underline{Z}_n); \quad \underline{Y}_g^1 = 1/\underline{Z}_g^1; \quad \underline{Y}_g^2 = 1/\underline{Z}_g^2, \quad (11)$$

where \underline{Z}_n is impedance between neutral and ground (SGs are usually directly grounded-Y, or $\underline{Z}_n = 0$) and \underline{Z}_g^0 (\underline{Z}_g^2) is zero (negative) sequence impedance.

The sequence models of the SG from Fig. 3 can be represented as

$$\mathbf{I}_g^{012} = [0 \ I_L \ 0]^T - \mathbf{Y}_g^{012} \mathbf{V}_g^{012}, \quad (12)$$

where

$$\mathbf{I}_g^{012} = [I_g^0 \ I_g^1 \ I_g^2]^T; \\ \mathbf{Y}_g^{012} = \text{diag}\{\underline{Y}_g^0, \underline{Y}_g^1, \underline{Y}_g^2\}; \\ \mathbf{V}_g^{012} = [V_g^0 \ V_g^1 \ V_g^2]^T.$$

The three-phase SG model can be obtained by transforming the sequence model (12) to the phase coordinates using the transformation matrix (\mathbf{A})

$$\mathbf{A} \mathbf{I}_g^{012} = \mathbf{A} [0 \ I_L \ 0]^T - \mathbf{A} \mathbf{Y}_g^{012} \mathbf{A}^{-1} \mathbf{A} \mathbf{V}_g^{012}, \quad (13)$$

or

$$\mathbf{I}_g = [1 \ a^2 \ a]^T I_L - \mathbf{Y}_g \mathbf{V}_g, \quad (14)$$

where

$$\mathbf{I}_g = [I_{ga} \ I_{gb} \ I_{gc}]^T = \mathbf{A} \mathbf{I}_g^{012};$$

$$\mathbf{Y}_g = \mathbf{A} \mathbf{Y}_g^{012} \mathbf{A}^{-1};$$

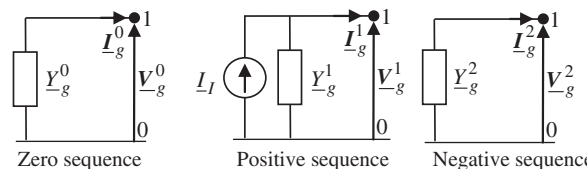


Fig. 3. The Norton equivalent sequence circuits of the SG with round-rotor.

Table 2
State variables and necessary measurements for DG bus observability.

Unit	State variables		Bus measurements			Internal power measurements	
	#	Type	#	Type	Description (for $\underline{S}_r = \mathbf{0}$)	#	Description and type
Synchronous generator (SG)	8	$\underline{V}_g, I_f = I_f^1$	6	rt	\underline{S}_g	2	$P_T(rt), Q_T(rt)$ $P_T(p), Q_T(p)$ (Sections 3.1 and 3.2)
Induction generator (IG)	7	\underline{V}_g, s	6	rt	\underline{S}_g	1	$P_T(rt)$ $P_T(p)$ (Sections 3.1 and 3.2)
			p	\underline{S}_g , Eq. (20)			
			v	$\underline{S} = \mathbf{0}$, Eq. (17)			
Three-wire VSC-coupled DG unit	10	$\underline{V}_g, I_f = I_f^1, I_f^2$	6	rt	\underline{S}_g	4	$P_T = P_T^1(rt), Q_T^1 = 0(v) P_T^2 = Q_T^2 = 0(v)$ $P_T = P_T^1(p), Q_T^1 = 0(v)$ (Sections 3.1 and 3.2) $P_T^2 = Q_T^2 = 0(v)$
			p	\underline{S}_g , From Eqs. (22)–(25)			
			v	$\underline{S} = \mathbf{0}$, Eq. (17)			
Four-wire VSC-coupled DG unit	8	$\underline{V}_g, I_f = I_f^1$	6	rt	\underline{S}_g	2	$P_T(rt), Q_T = 0(v)$ $P_T(p), Q_T = 0(v)$ (Sections 3.1 and 3.2)
			p	\underline{S}_g , From Eq. (25)			
			v	$\underline{S} = \mathbf{0}$, Eq. (17)			

$$\underline{V}_g = [\underline{V}_{ga} \quad \underline{V}_{gb} \quad \underline{V}_{gc}]^T = \underline{A}\mathbf{V}_g^{012}.$$

By multiplying the conjugated phase current from vector (14) on both sides by the phase voltages from vector \underline{V}_g , the three-phase apparent powers injected to the grid can be derived

$$\underline{S}_g = [\underline{S}_{ga} \quad \underline{S}_{gb} \quad \underline{S}_{gc}]^T = [\underline{S}_T \quad \underline{S}_T \quad \underline{S}_T]^T / 3 - (\underline{Y}_g^* \underline{V}_g^*) \times \underline{V}_g \quad (15)$$

and complex equation for internal SG apparent power is

$$\underline{S}_T = P_T + jQ_T = ([1 \quad a \quad a^2] I_f^*) \cdot \underline{V}_g. \quad (16)$$

Finally, the SG is modeled with the three-phase power balance equation at the bus where SG is connected to the grid

$$\underline{S} = \underline{S}_g - \underline{S}_T = (\underline{Y}_{BUS,g}^* \underline{V}_g^*) \times \underline{V}_g, \quad (17)$$

where \underline{S} is vector of injected three-phase apparent powers.

In the case where there is no load connected to the generator's bus ($\underline{S}_T = \mathbf{0}$ in (17)), the three-phase equality constraints (17) are treated as the virtual measurements in the SE algorithm (see Table 2).

Based on (16) and (17) three additional complex (or six real) phase voltage state variables (complex vector \underline{V}_g) for SG are introduced, at the bus where SG is connected to the grid and two additional internal state variables (complex current of Norton equivalent, I_f in Fig. 3). This means that for observability of the bus where the unmonitored SG is connected two additional (usually pseudo) measurements of real and reactive powers are needed (see Section 3 and Table 2).

2.4.2. SG with salient-poles

The SGs that are driven by water wheels in hydraulic turbines (hydro-generators) have laminated salient-pole rotors with concentric field windings and, usually, a large number of poles. This type of electric machines has different electric and magnetic properties on two axes 90° apart: (1) the direct (d) axis (axis of symmetry of a field pole) and (2) the quadrature (q) axis (axis of symmetry midway between two field poles). For effects of saliency to the parameters in the three-phase model from Fig. 3, see Ref. [23–Sec. 6].

2.4.3. Induction generator (IG) [11,15,23]

The sequence model of the IG from sequence equivalent circuits in Fig. 4 is

$$\underline{I}_g^{012} = \underline{Y}_g^{012} \underline{V}_g^{012}, \quad (18)$$

where

$$\underline{I}_g^{012} = [0 \quad I_g^1 \quad I_g^2]^T;$$

$$\underline{Y}_g^{012} = \text{diag}\{0, \underline{Y}_g^1, \underline{Y}_g^2\};$$

$$\underline{V}_g^{012} = [0 \quad \underline{V}_g^1 \quad \underline{V}_g^2]^T;$$

$$\underline{Y}_g^1 = \frac{1}{\underline{Z}_s + (\underline{Z}_r + R_r^1) \parallel \underline{Z}_m}; \quad \underline{Y}_g^2 = \frac{1}{\underline{Z}_s + (\underline{Z}_r + R_r^2) \parallel \underline{Z}_m};$$

$\underline{Z}_s, \underline{Z}_r = (R_r + jX_r), \underline{Z}_m$ is the stator, rotor and magnetizing impedances, respectively.

The three-phase IG model can be derived by transforming the sequence model (18) to the phase coordinates using the transformation matrix (\underline{A})

$$\underline{A}\underline{I}_g^{012} = \underline{A}\underline{Y}_g^{012}\underline{A}^{-1}\underline{A}\underline{V}_g^{012}, \text{ or } \underline{I}_g = \underline{Y}_g \underline{V}_g. \quad (19)$$

where $\underline{I}_g, \underline{V}_g$ and \underline{Y}_g are defined similarly as in (14).

Similarly as in (15), by multiplying the conjugated phase current from vector (19) on both sides by the phase voltages from vector \underline{V}_g , the three-phase apparent powers injected to the grid can be derived

$$\underline{S}_g = [\underline{S}_{ga} \quad \underline{S}_{gb} \quad \underline{S}_{gc}]^T = \underline{I}_g^* \times \underline{V}_g = (\underline{Y}_g^* \underline{V}_g^*) \times \underline{V}_g. \quad (20)$$

Finally, similarly as in (17), the IG is modeled with three-phase power balance equation in bus where IG is connected to the grid.

Internal real power of the IG is

$$P_T = P_T^1 + P_T^2 = -3R_r^1(I_r^1)^2 - 3R_r^2(I_r^2)^2, \quad (21)$$

where

$$I_r^{1(2)} = -\frac{\underline{Z}_m}{(R_r^{1(2)} + \underline{Z}_r)(\underline{Z}_m + \underline{Z}_s) + \underline{Z}_s \underline{Z}_m} \underline{V}_g^{1(2)};$$

$$R_r^1 = R_r \frac{1-s}{s}; \quad R_r^2 = R_r \frac{-(1-s)}{2-s};$$

$$\underline{V}_g^1 = \frac{1}{3}(\underline{V}_a + a\underline{V}_b + a^2\underline{V}_c); \quad \underline{V}_g^2 = \frac{1}{3}(\underline{V}_a + a^2\underline{V}_b + a\underline{V}_c).$$

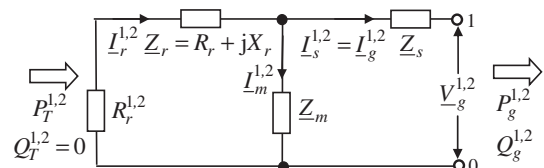


Fig. 4. The IG positive and negative sequence equivalent circuits [23–Sec. 6].

Based on (20) and (21) three complex (or six real) phase voltage state variables (complex vector \underline{V}_g) for IG are introduced, at the bus where IG is connected to the grid and one additional internal state variable (slip of the IG). This means that for observability of the bus where the unmonitored IG is connected only one additional (usually pseudo) measurement of real power (21) is requested (see Section 3 and Table 2).

2.4.4. Three-phase electronically-coupled DG unit

Zero, positive and negative sequence Norton equivalent circuits of the three-phase electronically-coupled DG unit are interfaced via a three-phase, three-wire (four-wire) voltage-sourced converter (VSC), are shown in Fig. 5. It is assumed that the VSC tightly regulates the DC-link voltage, and thus the primary source does not affect the steady-state model of the unit with respect to its point of connection to the grid.

2.4.4.1. Three-wire VSC-coupled DG unit [15 and Refs. therein]. If a three-wire interface-VSC is controlled only based on the positive sequence d - q current control method, the DG unit also exchanges negative sequence current with the network when the network is not balanced (i.e., when it includes negative sequence components). In this case, the positive, zero and negative sequence components of the model are specified as

$$\underline{I}_f^1 = \underline{I}_f; \quad \underline{I}_f^{0,2} = 0; \quad \underline{Y}_g^0 = 0; \quad \underline{Y}_g^2 = 1/\underline{Z}_f, \quad (22)$$

where \underline{Z}_f is the equivalent series impedance of the VSC output filter between the point of common coupling and the short-circuited VSC terminals.

If a three-wire interface-VSC is equipped with both positive and negative sequence current control schemes, and the negative sequence current control is assigned to prevent negative sequence current exchange with the network, then the positive, zero and negative sequence models are defined as

$$\underline{I}_f^1 = \underline{I}_f; \quad \underline{I}_f^{0,2} = 0; \quad \underline{Y}_g^{0,2} = 0. \quad (23)$$

For some applications, the negative sequence controller of the interface-VSC is used to inject a pre-specified negative sequence current to the grid, for example, for islanding detection. In this case, the zero, positive and negative sequence models of the interface-VSC are

$$\underline{I}_f^0 = 0; \quad \underline{I}_f^1 = \underline{I}_f; \quad \underline{I}_f^2 = I_{NSCI}/\phi_{NSCI}; \quad \underline{Y}_g^{0,2} = 0, \quad (24)$$

where I_{NSCI} and ϕ_{NSCI} are the magnitude and phase angle of the pre-specified negative sequence current, respectively.

For a three-wire interface-VSC, the parameters of the zero sequence model are always zero, since there is no path for zero sequence current flow.

2.4.4.2. Four-wire VSC-coupled DG unit [15 and Refs. therein]. The split-capacitor and the four-leg interface-VSC configurations do enable neutral connection and establish a four-wire VSC system. If a four-wire VSC only injects a controlled positive sequence current in the grid and permits the system to determine the exchanged positive, zero and negative sequence current components, then the corresponding models are

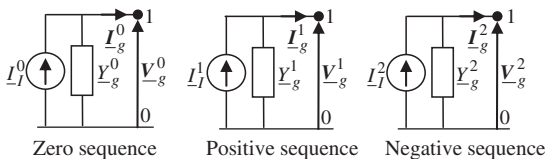


Fig. 5. The Norton equivalent circuits for three-phase electronically-coupled DG unit.

$$\underline{I}_f^1 = \underline{I}_f; \quad \underline{I}_f^{0,2} = 0; \quad \underline{Y}_g^0 = 1/(\underline{Z}_f + 3\underline{Z}_n); \quad \underline{Y}_g^2 = 1/\underline{Z}_f, \quad (25)$$

where \underline{Z}_n is impedance between neutral and ground.

Similarly as for SG (12)–(17), the three-phase voltage-current model for three-phase electronically-coupled DG unit, can be derived from the sequence models in Fig. 5 and (22)–(25).

3. State variables, bus observability and additional (pseudo) measurements

Different DG models (described in Section 2) introduce a new set of state variables and additional model based equations, as explained in Table 2. Sometimes, the DG units are unmonitored (or partially monitored), and therefore the bus observability is not satisfied. To provide the full DG bus observability, the additional set of real-time (rt), pseudo (p), or virtual (v) measurements in network buses with DGs installed, as well as and real-time and pseudo internal power measurements are requested. The internal active power is determined by the type of the DG unit (Section 3.1), while the internal reactive power is determined by the applied DG connection to the grid (Section 3.2).

3.1. Internal real power of the DG units [24 and Refs. therein]

For micro, small and medium hydro turbines without a reservoir the internal real power is extracted from the water flow as

$$P_h = P_T = \eta_h \rho_h g q_h h_h \quad (\text{kW}), \quad (26)$$

where η_h is the efficiency of the DG unit; ρ_h is the density of water ($\approx 1000 \text{ kg/m}^3$); g is the standard (Earth) gravity ($\approx 9.81 \text{ m/s}^2$); q_h is the flow of watercourse (m^3/s); and h_h is the water head (m).

For wind turbine the internal real power is extracted from the airflow as

$$P_{WT} = P_T = 0.5 \rho_a A_{WT} c_p(\lambda) v^3 \quad (\text{kW}), \quad (27)$$

where ρ_a is the density of air ($\approx 1.225 \text{ kg/m}^3$); A_{WT} is the rotor area of wind turbine (m^2); $c_p(\lambda)$ is the power coefficient, defined by a set of curves [25], and approximated by the following polynomial

$$c_p(\lambda) = \sum_{k=0}^n a_k \lambda^k, \quad (28)$$

with coefficients a_k obtained by a criterion of the minimum least-square deviations; λ is the tip speed ratio of wind turbine, defined as

$$\lambda = \omega_R R / v, \quad (29)$$

ω_R is the angular speed of wind turbine rotor (rad/s); R is the radius of rotor blades at wind turbine (m); v is the wind speed at the turbine blades (m/s).

For photovoltaic based DG unit the internal real power can be calculated as

$$P_{PV} = P_T = \eta_{PV} \Re \cos \gamma A_{PV} \quad (\text{kW}), \quad (30)$$

where η_{PV} is the efficiency of photovoltaic panel; \Re is the solar radiation (W/m^2); γ is the angle of incidence of photovoltaic panel; and A_{PV} is the area of photovoltaic panel (m^2).

For internal combustion engines, fuel cells, gas turbines and micro turbines (Table 1) the internal real power (P_T) and the engine speed are controlled by power electronics interface that optimizes the fuel usage. In our simulations for these units, it is assumed that the internal real power is equal to the rated power.

3.2. Internal reactive power of the DG units

For different connections of the DG unit to the grid, the internal reactive power (Q_T) can be calculated as:

SG based DG unit: In this case, Q_T can be adopted from P-Q diagram, respecting the internal real power (P_T) and the SG unit limits [26-Part I, Sec. 3].

IG based DG unit: In this case, the reactive power is taken from the grid (Q_g) to cover the reactive losses in equivalent circuit from Fig. 4, or $Q_T = 0$. Usually this configuration uses a capacitor bank for the reactive power compensation, where the compensation level can be calculated from SE results.

Electronically-coupled DG based unit: Similarly as for IG based DG units, in this case it is assumed that $Q_T = 0$ [15].

4. The WLS-based three-phase SE algorithm

The WLS-based algorithm for three-phase SE in active distribution networks is applied to minimize the objective function (real-time and pseudo-measurements based model) [27]

$$\min_{\mathbf{x}} \{ J(\mathbf{x}) = [\mathbf{z} - \mathbf{h}(\mathbf{x})]^T \mathbf{R}^{-1} [\mathbf{z} - \mathbf{h}(\mathbf{x})] \}, \quad (31)$$

subject to equality constraints (virtual measurements)

$$\mathbf{c}(\mathbf{x}) = \mathbf{0}, \quad (32)$$

where \mathbf{x} is the state vector composed from the components of complex voltage (phasor magnitudes and angles) and additional state variables depending on the type of DG unit (see Section 3 and Table 2); \mathbf{z} is the measurement vector; and $\mathbf{h}(\mathbf{x})$ is the measurements-state variables model (note that in $\mathbf{h}(\mathbf{x})$ are included in the additional equations and state variables for different applied DG unit models, as described in Section 2).

$\mathbf{R} = \text{diag}\{\sigma_1^2, \sigma_2^2, \dots, \sigma_M^2\}$, where σ is standard deviation and M is a total number of real-time and pseudo-measurements.

The WLS-based three-phase SE algorithm in active distribution network can be summarized in the following steps (Fig. 6):

Step 1a: - Set iteration count to $(k) = 0$.

- Calculate the initial state vector ($\mathbf{x}^{(k)}$) by symmetrical power flow.
- Define the subvector of real-time measurements (\mathbf{z}_{rt}).
- Identification of buses with zero injections (virtual measurements), that determines the set of equality constraints ($\mathbf{c}(\mathbf{x}) = \mathbf{0}$).

Step 1b: Load allocation (for real power with assumed constant power factor) for load buses from normalized daily load profiles (LP), respecting load, day and season type [24,28], and update these elements in vector of pseudo-measurements (\mathbf{z}_p).

- Real/Reactive power allocation for buses with DG units connected from external inputs (Section 3), and update these elements in vector of pseudo-measurements (\mathbf{z}_p).

Step 2: Calculate the increments of all measurements by

$$\Delta \mathbf{z}^{(k)} = \mathbf{z}^{(k)} - \mathbf{h}(\mathbf{x}^{(k)}), \quad (33)$$

Step 3: Calculate Jacobian $[\mathbf{H}(\mathbf{x}) = \partial \mathbf{h}(\mathbf{x}) / \partial \mathbf{x}$, $\mathbf{C}(\mathbf{x}) = \partial \mathbf{c}(\mathbf{x}) / \partial \mathbf{x}]$, and information $[\mathbf{G}(\mathbf{x}) = \mathbf{H}(\mathbf{x})^T \mathbf{R}^{-1} \mathbf{H}(\mathbf{x})]$ matrices in point $\mathbf{x} = \mathbf{x}^{(k)}$, as well as the increment of state vector ($\Delta \mathbf{x}^{(k)}$) from

$$\begin{bmatrix} \mathbf{G}(\mathbf{x}^{(k)}) & \mathbf{C}(\mathbf{x}^{(k)})^T \\ \mathbf{C}(\mathbf{x}^{(k)}) & \mathbf{0} \end{bmatrix} \begin{bmatrix} \Delta \mathbf{x}^{(k)} \\ -\lambda^{(k)} \end{bmatrix} = \begin{bmatrix} \mathbf{H}(\mathbf{x}^{(k)})^T \mathbf{R}^{-1} \Delta \mathbf{z}^{(k)} \\ -\mathbf{c}(\mathbf{x}^{(k)}) \end{bmatrix}, \quad (34)$$

Step 4: Check the convergence criterion

$$\max |\Delta x_x^{(k)}| \leq \varepsilon, \quad k = 1, 2, \dots, K, \quad (35)$$

where K is a total number of state variables and ε is a convergence criterion.

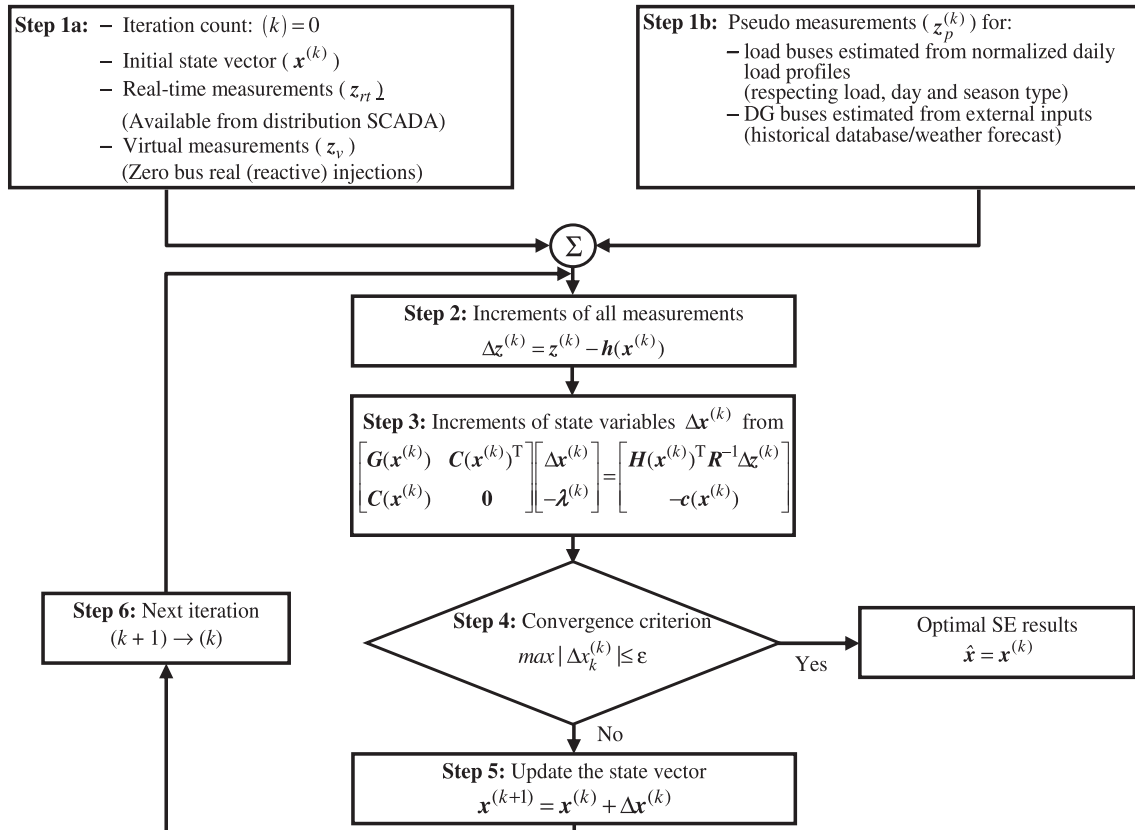


Fig. 6. Flow-chart of the proposed algorithm for three-phase SE algorithm in active distribution networks.

If criterion (34) is satisfied, then $\hat{\mathbf{x}} = \mathbf{x}^{(k)}$, and Go to STOP, Else Continue.

Step 5: Update the state vector

$$\mathbf{x}^{(k+1)} = \mathbf{x}^{(k)} + \Delta \mathbf{x}^{(k)}, \tag{36}$$

Step 6: $(k + 1) \rightarrow (k)$ and Go to Step 2.

In general, the three-phase SE algorithm for unbalanced active distribution networks has about three times more state variables, compared with the single-phase SE algorithm (depending on network topology and participation of the single and two phase laterals), but it does not have significant influence to the convergence (number of iterations) of the proposed algorithm (see Section 5).

5. Application

The proposed three-phase SE algorithm in unbalanced active distribution networks is tested on two characteristic examples. The first example is the IEEE 13-bus test system, for which all the simulation details with an analysis of observed physical laws are provided. For the 322-bus 110/35/10/0.4 kV real-world distribution network, only performance results of the proposed SE algorithm are provided, with paying attention to the applicability to large-scale distribution network.

Explained algorithm does not perform corrections of assumed Gaussian distribution of pseudo-measurements (mean and variance), respecting the calculated state variables (operating condition) of the distribution networks (load/generation reallocation procedure). Sometimes the reallocation procedure can filter the inconsistencies between real-time and pseudo-measurements, and consequently improve the estimations results [24]. This procedure, originally proposed for single-phase SE can be included in the proposed three-phase SE without theoretical and/or practical constraints.

5.1. Modified IEEE 13-bus test system [29]

This is an unbalanced 4.16 kV radial distribution network with minimally modified input bus data, where three DGs were added in buses 5, 8 and 13, as shown in the three-phase diagram in Fig. 7. The modified bus load/generation and power flow real-time/pseudo-measurements are presented in Table 3.

Standard deviation (σ) of real-time/pseudo measurement is calculated from measurement mean value and accuracy (A_c) as [22,24].

$$\sigma = \text{Mean} \cdot (A_c/300), \tag{37}$$

where assumed accuracies in simulation tests are: $A_{c_{rt}} = 3\%$ and $A_{c_p} = 20\%$.

For load condition given in Table 3 and feeder denoted by dotted line in Fig. 7, the initial and the estimated three-phase real powers in load/generation buses (with real-time or pseudo-measurements) are shown in Fig. 8. Estimated bus voltage phasors and phase voltage deviations (from the rated phase voltage) are shown in Fig. 9. The convergence criterion in SE algorithm ($\varepsilon = 1 \times 10^{-4}$) was reached after three iterations.

In this case, the single-phase lines/loads significantly increases the average voltage imbalance factors, where average values are $V^2/V^1 = 26.95\%$ and $V^0/V^1 = 27.15\%$ (see Section 5.2).

5.2. 322-Bus real-world distribution network [24]

This is an unbalanced 110/35/10/0.4 kV real-world distribution network.

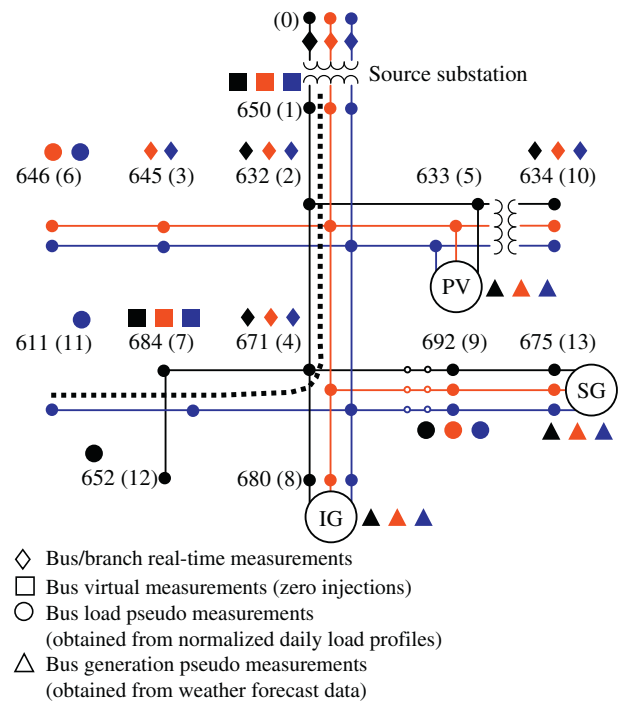


Fig. 7. Three-phase topology of the modified IEEE 13-bus test system.

Table 3 Bus load/generation and power flow real-time (rt) and pseudo (p) measurements.

Bus/branch	Measurement type	Phase a		Phase b		Phase c	
		(kW)	(kV Ar)	(kW)	(kV Ar)	(kW)	(kV Ar)
2	rt	8.5	19.0	5.0	58.5	33.0	34.0
3	rt	-	-	170.0	125.0	-	-
4	rt	393.5	239.0	390.0	278.5	418.0	254.0
5	p (SG)	-10.0	0.0	-10.0	0.0	-10.0	0.0
6	p (LP)	-	-	115.0	66.0	115.0	66.0
8	p (IG)	-16.7	-3.3	-16.7	-3.3	-16.7	-3.3
9	p (LP)	86.7	44.0	86.7	44.0	86.7	44.0
10	rt	160.0	110.0	120.0	90.0	120.0	90.0
11	p (LP)	-	-	-	-	170.0	80.0
12	p (LP)	128.0	86.0	-	-	-	-
13	p (PV)	-30.0	-10.0	-30.0	-10.0	-30.0	-10.0
0-1	rt	810.0	490.0	910.0	660.0	970.0	510.0

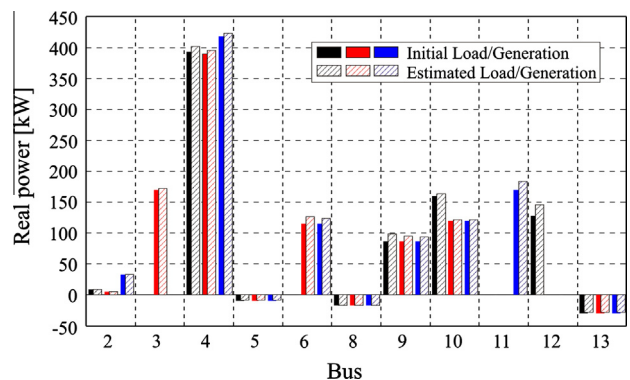


Fig. 8. Initial and estimated three-phase real power in load/generation buses with real-time and pseudo-measurements.

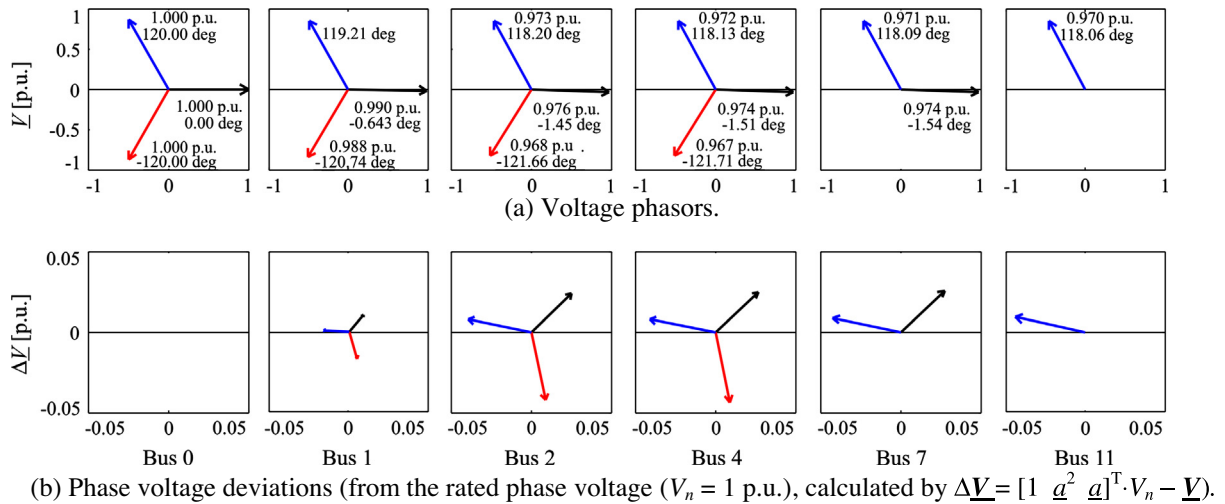


Fig. 9. Estimated voltage phasors in buses.

Table 4

Maximum and average voltage imbalance factors for different random variations of loads.

Maximum and average imbalance factors (%)	Random load variation (%)			
	Base case	±10	±20	±30
Max $\{V^2/V^1\}$	3.06×10^{-7}	2.43×10^{-2}	5.47×10^{-2}	6.16×10^{-2}
Max $\{V^0/V^1\}$	9.48×10^{-7}	2.66×10^{-2}	4.56×10^{-2}	7.48×10^{-2}
Average $\{V^2/V^1\}$	2.29×10^{-7}	5.31×10^{-3}	1.57×10^{-2}	1.37×10^{-2}
Average $\{V^0/V^1\}$	1.25×10^{-7}	7.18×10^{-3}	1.09×10^{-2}	1.55×10^{-2}

The total number of available real-time measurement places (with paired real/reactive power injections or power flow measurements) is 17, distributed on:

- 2 Substations 110/36.75 kV and 14 substations 35/10.5 kV.
- 1 Load bus (industry complex).

Initial system's total real load is 8.80 p.u., where all p.u. values are referenced to the base power of 3 MVA.

The available unmonitored DGs are:

- Five wind generators with the same technical characteristics and initial total internal real power output 0.17 p.u. (initial estimation based on the weather forecast).
- One photovoltaic unit with assumed the internal real power output 0.01 p.u. (initial estimation based on the weather forecast).
- One gas turbine with assumed the internal (rated) power 0.2 p.u.
- The convergence criterion ($\varepsilon = 1 \times 10^{-4}$) is reached after seven iterations.

Influence on different random variations in three-phase unbalanced loads (from balanced base case) on the voltage imbalance factors is presented in Table 4.

6. Conclusion

In this paper, the Weighted Least Square (WLS) based state estimation algorithm for unbalanced active distribution networks was proposed and verified on two characteristic test examples. The proposed model accommodates the different configurations

of three-phase transformers, lines, loads and distribution generation (DG) units.

By conducting the extensive simulation studies, with different number, type and locations of real-time, virtual and pseudo-measurements, we can conclude that the algorithm is robust and efficient for application in Distribution Management System. Performed and presented numerical tests show that asymmetry of the distribution network conditions can be significant in the real-world operation, disregarding the application of single-phase state estimation algorithms. In addition, the detailed modeling of different DG types (including their connection to the grid) is very important for the estimation of losses and asymmetry between the internal and output variables (voltages and real/reactive powers).

Acknowledgement

The authors thank to the Ministry of Education and Science of the Republic of Serbia for its support of this work provided within Projects III-42004 and III-42009.

Appendix A. Three-phase transformer model [11,12]

Table A1 shows the transformer submatrices from Fig. 1 for the common step-down three-phase transformer connections (to simplify the presentation, the neutral transformer tap changer position is assumed) where particular submatrices in Table A1 are defined as

$$\underline{Y}_I = \begin{bmatrix} 1 & 0 & 0 \\ 0 & 1 & 0 \\ 0 & 0 & 1 \end{bmatrix} \begin{bmatrix} \underline{Y}_{sc} \\ \underline{Y}_{sc} \\ \underline{Y}_{sc+n} \end{bmatrix}; \quad \underline{Y}_{II} = \frac{1}{3} \begin{bmatrix} 2 & -1 & -1 \\ -1 & 2 & -1 \\ -1 & -1 & 2 \end{bmatrix} \underline{Y}_{sc};$$

$$\underline{Y}_{III} = \frac{1}{\sqrt{3}} \begin{bmatrix} -1 & 1 & 0 \\ 0 & -1 & 1 \\ 1 & 0 & -1 \end{bmatrix} \underline{Y}_{sc},$$
(A1)

Table A1

Transformer submatrices (\underline{Y}_T) for common three phase step-down transformer connections [11,12].

Connection	\underline{Y}_{pp}	\underline{Y}_{ps}	\underline{Y}_{sp}	\underline{Y}_{ss}
Y_{NY_n}	\underline{Y}_I	$-\underline{Y}_I$	$-\underline{Y}_I$	\underline{Y}_I
$Y_{NY}, Y_{y_n}, Y_y, D_d$	\underline{Y}_{II}	$-\underline{Y}_{II}$	$-\underline{Y}_{II}$	\underline{Y}_{II}
Y_{Nd}	\underline{Y}_I	\underline{Y}_{II}^T	\underline{Y}_{III}	\underline{Y}_{II}
Y_d, D_y	\underline{Y}_{II}	\underline{Y}_{II}^T	\underline{Y}_{III}	\underline{Y}_{II}
D_{y_n}	\underline{Y}_{II}	\underline{Y}_{II}^T	\underline{Y}_{III}	\underline{Y}_I

where

$$\underline{Y}_{sc} = 1/\underline{Z}_{sc}; \quad \underline{Y}_{sc+n} = 1/(\underline{Z}_{sc} + 3\underline{Z}_n);$$

\underline{Z}_{sc} is the short circuit admittance and \underline{Z}_n is the impedance between neutral and ground (for directly grounded transformer is $\underline{Z}_n = 0$).

Matrix \underline{Y}_I is regular, while \underline{Y}_{II} and \underline{Y}_{III} are singular matrices. Furthermore, based on Table A1, depending on connection type, the matrices \underline{Y}_{pp} , \underline{Y}_{ps} , \underline{Y}_{sp} and \underline{Y}_{ss} can be regular or singular, where singular matrices are not a constraint for the application of proposed SE algorithm, because the symmetrical initial phase voltages for calculation of matrices \underline{H} and \underline{C} (Step 3 in Section 4) are assumed.

References

- [1] Abur A, Exposito AG. Power system state estimation: theory and implementation. Marcel Dekker; 2004.
- [2] Singh R, Pal BC, Jabr RA. Choice of estimator for distribution system state estimation. IET Gener Transm Distrib 2009;152:240–6.
- [3] Farantatos E, Huang R, Cokkinides GJ, Meliopoulos AP. Implementation of a 3-phase state estimation tool suitable for advanced distribution management systems. IEEE/PES Power Syst Conf Expos (PSC) 2011;1:1–8.
- [4] Lu CN, Teng JH, Liu W-HE. Distribution system state estimation. IEEE Trans Power Syst 1995;10:229–40.
- [5] Meliopoulos AP, Cokkinides GJ, Stefopoulos GK. Numerical experiments for three-phase state estimation performance and evaluation. Power Tech IEEE Russ 2005;1:1–7.
- [6] Wu W, Ju Y, Zhang B, Sun H. A distribution system state estimator accommodating large number of ampere measurements. Int J Electr Power Energy Syst 2012;43:839–48.
- [7] Thornley V, Jenkins N, White S. State estimation applied to active distribution networks with minimal measurements. In: 15th PSCC conference, Liege, vol. 1; 2005. p. 1–7.
- [8] Li K. State estimation for power distribution system and measurement impacts. IEEE Trans Power Syst 1996;11:911–6.
- [9] Haibin W, Schulz NN. A revised branch current-based distribution system state estimation algorithm and meter placement impact. IEEE Trans Power Syst 2004;19:207–13.
- [10] Lubkeman DL, Jianzhong Z, Ghosh AK, Jones RH. Field results for a distribution circuit state estimator implementation. IEEE Trans Power Deliv 2000;15:399–406.
- [11] Chen TH, Chen MS, Inoue T, Kotas P, Chebli EA. Three-phase cogenerator and transformer models for distribution system analysis. IEEE Trans Power Deliv 1991;6:1671–81.
- [12] Xiao P, Yu DC, Yan W. A unified three-phase transformer model for distribution load flow calculations. IEEE Trans Power Syst 2006;21:153–9.
- [13] Singh S, Ghose T. Improved radial load flow method. Int J Electr Power Energy Syst 2013;44:721–7.
- [14] Strezoski VC, Trpezanovski Lj. Three-phase asymmetrical load-flow. Int J Electr Power Energy Syst 2000;22:511–20.
- [15] Kamh MZ, Iravani R. A unified three-phase power-flow analysis model for electronically coupled distributed energy resources. IEEE Trans Power Deliv 2011;26:899–909.
- [16] Araujo LR, Penido DRR, Vieira FA. A multiphase optimal power flow algorithm for unbalanced distribution systems. Int J Electr Power Energy Syst 2013;53:632–42.
- [17] Abbasi AR, Seifi AR. A new coordinated approach to state estimation in integrated power systems. Int J Electr Power Energy Syst 2013;45:152–8.
- [18] Hansen CW, Debs AS. Power system state estimation using three-phase models. IEEE Trans Power Syst 1995;10:818–24.
- [19] Kersting WH. Distribution system modeling and analysis. CRC Press; 2002.
- [20] Zhu Y, Tomovic K. Adaptive power flow method for distribution systems with dispersed generation. IEEE Trans Power Deliv 2002;17:822–7.
- [21] Tafreshi SMM, Mashhour E. Distributed generation modeling for power flow studies and a three-phase unbalanced power flow solution for radial distribution systems considering distributed generation. Electr Power Syst Res 2009;79:680–6.
- [22] Cobelo I, Shafiu A, Jenkins N, Strbac G. State estimation of networks with distributed generation. Eur Trans Electr Power 2007;17:21–36.
- [23] Anderson PM. Analysis of faulted power systems. John Wiley and Sons; 1995.
- [24] Sarić AT, Ranković A. Load reallocation based algorithm for state estimation in distribution networks with distributed generators. Electr Power Syst Res 2012;84:77–82.
- [25] Fox B, Flynn D, Bryans L, Jenkins N. Wind power integration: connection and system operational aspects. London, UK: IEE; 2007.
- [26] Machowski J, Bialek JW, Bumby JR. Power systems dynamics and stability. 2nd ed. Wiley; 2008.
- [27] Korres GN. A robust method for equality constrained state estimation. IEEE Trans Power Syst 2002;17:305–14.
- [28] Sarić AT, Čirić RM. Integrated fuzzy state estimation and load flow analysis in distribution networks. IEEE Trans Power Deliv 2003;18:571–8.
- [29] <http://ewh.ieee.org/soc/pes/dsacom/testfeeders/index.html>; 2013 [accessed 01.07.13].